Superfluid Density in the $s_\pm$-Wave State of Clean Iron-Based Superconductors

Huaixiang Huang,[1,2] Yi Gao,[3] Jian-Xin Zhu,[4] and C. S. Ting[2]

[1]*Department of Physics, Shanghai University, Shanghai 200444, China*
[2]*Texas Center for Superconductivity and Department of Physics, University of Houston, Houston, Texas 77204, USA*
[3]*Department of Physics and Institute of Theoretical Physics, Nanjing Normal University, Nanjing, Jiangsu 210046, China*
[4]*Theoretical Division and Center for Integrated Nanotechnologies, Los Alamos National Laboratory, Los Alamos, New Mexico 87545, USA*
(Received 3 May 2012; published 2 November 2012)

Based on a phenomenological model and the Kubo formula, we investigate the superfluid density $\rho_s(T)$ and then the penetration depth $\lambda(T)$ of the iron-based superconductors in the coexistence region of the spin-density wave and superconductivity, and also in the overdoped region. Our calculations show a dramatic increase of $\lambda(0)$ with the decrease of the doping concentration x below $x = 0.1$. This result is consistent with the experimental observations. At low temperatures, $\rho_s(T)$ shows an exponential-law behavior, while at higher temperatures, the linear-in-T behavior is dominant before it trends to vanish. It is in qualitative agreement with the direct measurement of superfluid density in films of Fe-pnictide superconductor at $x = 0.08$. The evolution of $\Delta\lambda(T)$ can be roughly fitted by a power-law function with the exponent depending on the doping concentration. We show that the Uemura relation holds for the iron-based superconductors only at very low doping levels.

In addition to zero resistance, the Meissner effect is another hallmark of superconductivity. The directly measured penetration depth (λ) in a weak magnetic field provides information of the gap structure, and is a characteristic length scale of a bulk superconductor. In general, $\rho_s \propto 1/\lambda^2$. The number of electrons in the superconducting phase, ρ_s, characterizes the phase rigidity of a superconductor. In conventional Bardeen-Cooper-Schrieffer superconductors, the penetration depth exhibits an exponential behavior at low temperatures, and the power-law behavior in $\Delta\lambda(T) \equiv \lambda(T) - \lambda(0)$ has been considered as evidence for unconventional pairing symmetry in the high-temperature superconductors [1]. Compare to cuprates, the remarkable features of iron pnictides are the nature of magnetism and the multiband character. They have triggered massive studies since their discovery [2,3]. In this Letter we focus on its response to a weak external magnetic field.

There are several ways to measure magnetic penetration depth [4–6]. In the 1111 systems, at low temperatures, some experiments [7] found a power-law behavior $\lambda(T)$, while others [8,9] have found an exponential temperature dependence of $\lambda(T)$. The situation in the 122 system is also unclear: The superfluid density $\rho_s(T)$ exhibits an exponential behavior in the cleanest $Ba_{1-x}K_xFe_2As_2$ [10], while measurements on $Ba(Fe_{1-x}Co_x)_2As_2$ have shown a power-law behavior of $\lambda(T)$ [11–16] with the exponent varying from 1.6 to 2.8, and a two-gap scenario is suggested for $Ba(Fe_{1-x}Co_x)_2As_2$ and $Ba_{1-x}Rb_xFe_2As_2$ [17,18]. And there are also some theoretical works [19–22].

In this Letter, we carry out systematic calculations of $\rho_s(T)$ based on a two-orbital phenomenological model [23]. Within this model, each unit cell accommodates two inequivalent Fe ions and results based on this model on various properties of Fe-pnictide superconductors [23–31] are in reasonable agreement with experimental measurements. When we normalize the energy parameters of the Fe-Fe nearest and next-nearest neighbors, the hopping integrals defined below are chosen as $t_{1-4} = 1, 0.4, -2.0, 0.04$ [23], respectively. In the momentum k space, the single-particle Hamiltonian matrix can be written as [26,27]

$$H_{t,k} = \begin{pmatrix} a_1 - \mu & a_3 & a_4 & 0 \\ a_3 & a_1 - \mu & 0 & a_4 \\ a_4 & 0 & a_2 - \mu & a_3 \\ 0 & a_4 & a_3 & a_2 - \mu \end{pmatrix}, \quad (1)$$

with $a_1 = -2t_2\cos(k_x + k_y) - 2t_3\cos(k_x - k_y)$, $a_2 = -2t_3\cos(k_x - k_y) - 2t_2\cos(k_x + k_y)$, $a_3 = -2t_4(\cos(k_x + k_y) + \cos(k_x - k_y))$, $a_4 = -2t_1(\cos k_x + \cos k_y)$, where μ is the chemical potential. Here we have chosen the x axis along the link connecting nearest neighbor Fe ions, and the distance between nearest neighbor Fe is taken as the unit of length. The pairing term $H_{\Delta,k} = \sum_{\alpha\nu\mathbf{k}}(\Delta_{\alpha,\mathbf{k}} c^\dagger_{\alpha\nu\mathbf{k}\uparrow} c^\dagger_{\alpha\nu-\mathbf{k}\downarrow} +$ H.c.) has only next-nearest-neighbor intra-orbital pairing, where α denotes Fe A or Fe B in the unit cell and ν denotes the orbitals. It will lead to the $s_\pm$-wave pairing symmetry [10,11,32]. The self-consistent conditions are $\Delta_{\alpha\mathbf{k}} = 2\sum_\tau \cos k_\tau \Delta^\alpha_{i,i+\tau}$ and $\Delta^\alpha_{i,i+\tau} = \frac{V}{2}\langle c^\alpha_{i\nu\uparrow} c^\alpha_{i+\tau,\nu\downarrow} - c^\alpha_{i\nu\downarrow} c^\alpha_{i+\tau,\nu\uparrow}\rangle = \frac{V}{N_s}\sum_\mathbf{k} \cos k_\tau \langle c_{\alpha\nu,\mathbf{k}\uparrow} c_{\alpha\nu,-\mathbf{k}\downarrow}\rangle$, with $\tau = \mathbf{x} \pm \mathbf{y}$ and the pairing strength $V = 1.2$. The interaction term includes the Hund's coupling $J_H = 1.3$ and the on-site Coulomb interaction U, in which we choose $U = 3.4$ and $U = 4.0$ as two different kinds of homogenous systems. After taking the mean-field treatment [24,25], H_{int} can be expressed as

$$H_{\text{int}} = U \sum_{i\mu\sigma\neq\bar{\sigma}} \langle n_{i\mu\bar{\sigma}}\rangle n_{i\mu\sigma} + (U - 3J_H) \sum_{i\mu\neq\nu\sigma} \langle n_{i\mu\sigma}\rangle n_{i\nu\sigma}$$
$$+ (U - 2J_H) \sum_{i\mu\neq\nu\sigma\neq\bar{\sigma}} \langle n_{i\mu\bar{\sigma}}\rangle n_{i\nu\sigma}. \quad (2)$$

In the presence of spin-density-wave (SDW) order, H_{int} in the k space can be decoupled into a diagonal term and magnetic term. Define $\psi_{\mathbf{k}\sigma}^{\dagger} = (c_{A0,\mathbf{k}\uparrow}^{\dagger}, c_{A1,\mathbf{k}\uparrow}^{\dagger}, c_{B0,\mathbf{k}\uparrow}^{\dagger}, c_{B1,\mathbf{k}\uparrow}^{\dagger})$, $\varphi_{\mathbf{k}}^{\dagger} = (\psi_{\mathbf{k}\uparrow}^{\dagger}, \psi_{\mathbf{k}+\mathbf{Q}\uparrow}^{\dagger}, \psi_{-\mathbf{k}\downarrow}, \psi_{-\mathbf{k}+\mathbf{Q}\downarrow})$, the Hamiltonian without external field in k space can be written as $\varphi_{\mathbf{k}}^{\dagger} H_0 \varphi_{\mathbf{k}}$ [26,27], with

$$H_0 = \begin{pmatrix} H'_{t,\mathbf{k}} & R & IH_{\Delta,\mathbf{k}} & 0 \\ R & H'_{t,\mathbf{k}+\mathbf{Q}} & 0 & IH_{\Delta,\mathbf{k}+\mathbf{Q}} \\ IH_{\Delta,\mathbf{k}} & 0 & -H'_{t,\mathbf{k}} & R \\ 0 & IH_{\Delta,\mathbf{k}+\mathbf{Q}} & R & -H'_{t,\mathbf{k}+\mathbf{Q}} \end{pmatrix}, \quad (3)$$

where I is a 4×4 unit matrix, $R = -\frac{M}{2}(U + J_H)H_M$, and the corresponding $H'_{t,\mathbf{k}} = H_{t,\mathbf{k}} + \frac{n}{4}(3U - 5J_H)I$, with $n = 2 + x$. R relates to the magnetic order [26,27] with

$$H_M = \begin{pmatrix} I & 0 \\ 0 & I \exp i\mathbf{Q} \cdot \mathbf{R}_{AB} \end{pmatrix}, \quad (4)$$

in Eq. (4) I is a 2×2 unit matrix. Due to SDW order, the wave vector $\mathbf{k}$ is restricted in the magnetic Brillouin zone (BZ). The self-consistent condition is $M = \frac{1}{2}\sum_{\nu}(n_{A\nu\uparrow} - n_{A\nu\downarrow}) = \frac{1}{2N_s}\sum_{\nu,\mathbf{k}}\sigma c_{A\nu\sigma\mathbf{k}}^{\dagger} c_{A\nu\sigma\mathbf{k}+\mathbf{Q}}$, $\mathbf{R}_{AB}$ is the distance of Fe B to the origin sited by Fe A. N_s is the number of unit cells. We take $N_s = 512$ to obtain self-consistent parameters and $N_s = 768$ in the calculation of ρ_s. After diagonalizing $\sum_{\mathbf{k}}\varphi_{\mathbf{k}}^{\dagger} H_0 \varphi_{\mathbf{k}} = \sum_{\mathbf{k}m}E_{\mathbf{k},m}\gamma_m^{\dagger\mathbf{k}}\gamma_m^{\mathbf{k}}$ by a 16×16 canonical transformation matrix $\mathbb{T}$, we can obtain all properties of the system without the external field.

Our investigation of the superfluid density ρ_s follows the linear response approach described by Refs. [1,33–35]. In the presence of a slowly varying vector potential $A_x(r, t) = A(q, \omega)e^{i\mathbf{q}\cdot r_i - i\omega t}$ along the x direction, the hopping term is modified by a phase factor, $c_{i\sigma}^{\dagger} c_{j\sigma} \rightarrow c_{i\sigma}^{\dagger} c_{j\sigma} \exp i\frac{e}{\hbar c} \times \int_{r_j}^{r_i}\mathbf{A}(\mathbf{r}, t) \cdot d\mathbf{r}$. Throughout the Letter we set $\hbar = c = 1$. By expanding the factors to the order of A^2, we obtained the total Hamiltonian $H_{\text{tot}} = H_0 + H'$ with

$$H' = -\sum_i A_x(r_i, t)\left[eJ_x^P(r_i) + \frac{1}{2}e^2 A_x(r_i, t)K_x(r_i)\right]. \quad (5)$$

$J_x^P(r_i)$ is the particle current density along the x axis, $K_x(r_i)$ is the kinetic energy density along the x axis. Their expressions are

$$K_x(r_i) = -\sum_{\nu\nu'\sigma\delta} t_{i,i+\delta} x_{i,i+\delta}^2 (c_{i\nu\sigma}^{\dagger} c_{i+\delta,\nu'\sigma} + \text{H.c.}), \quad (6)$$

$$J_x^P(r_i) = -i\sum_{\nu\nu'\sigma\delta} t_{i,i+\delta} x_{i,i+\delta} (c_{i\nu\sigma}^{\dagger} c_{i+\delta,\nu'\sigma} - \text{H.c.}), \quad (7)$$

only $\delta = x, x \pm y$ have contributions to the x component and $x_{i,i+\delta} = 1$ in our coordination. The charge current density along the x axis is defined as

$$J_x^Q(r_i) \equiv -\frac{\delta H'}{\delta A_x(r_i, t)} = eJ_x^P(r_i) + e^2 K_x(r_i)A_x(r_i, t). \quad (8)$$

The kinetic energy is calculated to zeroth order of $A_x(r_i)$, corresponding to the diamagnetic part, and that of the paramagnetic part $J_x^P(r_i)$ is calculated to the first order of $A_x(r_i)$. In the interaction representation we have

$$\langle J_x^P(r_i)\rangle = -i\int_{-\infty}^{t} \langle [J_x^P(r_i, t), H'(t')]_{-}\rangle_0 dt'$$
$$= -\frac{eA_x(r, t)}{N_s}\Pi_{xx}(\mathbf{q}, \omega), \quad (9)$$

where $\langle\rangle$ represents the expectation value based on the wave function of H_{tot} while $\langle\rangle_0$ corresponds to the wave function of H_0. In the Matsubara formalism we have the current-current correlation $\Pi_{xx}(\mathbf{q}, i\omega) = \int_0^{\beta} d\tau e^{i\omega\tau}\Pi_{xx}(\mathbf{q}, \tau)$, and $\Pi_{xx}(\mathbf{q}, \tau) = -\langle T_{\tau}J_x^P(\mathbf{q}, \tau) \times J_x^P(-\mathbf{q}, 0)\rangle_0 = \sum_{m_1 m_2}\Pi_{xx}^{m_1 m_2}(\mathbf{q}, \tau)$ where T_{τ} is the time ordering operator, $J_x^P(\mathbf{q}, \tau) = e^{\tau H_0}J_x^P(\mathbf{q})e^{-\tau H_0}$, $J_x^P(\mathbf{q}) = \sum_i e^{-i\mathbf{q}\cdot r_i}J_x^P(r_i) = \sum_{m_1 m_2}J_{m_1,m_2}^P(\mathbf{q})$ is a summation over $\mathbf{k}$. Calculation of $\Pi_{xx}(\mathbf{q}, i\omega)$ is in the framework of equations of motion of Green's function,

$$\frac{d\Pi_{xx}^{m_1 m_2}(\mathbf{q}, \tau)}{d\tau} = -[J_{m_1,m_2}^P(\mathbf{q}), J_x^P(-\mathbf{q})]_{-}$$
$$- \langle T_{\tau}e^{H_0\tau}[H_0, J_{m_1,m_2}^P(\mathbf{q})]_{-}e^{-H_0\tau}J_x^P(-\mathbf{q}, 0)\rangle_0.$$

A lengthy but straightforward algebra leads to

$$\Pi_{xx}(\mathbf{q}, i\omega) = \sum_{\mathbf{k}m_1 m_2} \frac{Y_{m_1 m_2}^{\mathbf{k},\mathbf{k}+\mathbf{q}} Y_{m_2 m_1}^{\mathbf{k}+\mathbf{q},\mathbf{k}}(f(E_{\mathbf{k},m_1}) - f(E_{\mathbf{k}+\mathbf{q},m_2}))}{i\omega + (E_{\mathbf{k},m_1} - E_{\mathbf{k}+\mathbf{q},m_2})}, \quad (10)$$

where f is the Fermi distribution function. Through analytic continuation, $\Pi_{xx}(\mathbf{q}, \omega)$ is obtained. When $\omega = 0$, the derivative of f has an important contribution to $\Pi_{xx}(q, i\omega)$. The quantity $Y_{m_1 m_2}^{\mathbf{k},\mathbf{k}+\mathbf{q}}$ can be expressed as

$$Y_{m_1 m_2}^{\mathbf{k},\mathbf{k+q}} = \frac{2}{N_s}[t_4(\xi_4(\sin k_{x-y} + \sin k_{x+y}) + \xi_4'(\sin k_{x-y}^{\mathbf{Q}} + \sin k_{x+y}^{\mathbf{Q}}))$$
$$+ t_3(\xi_2 \sin k_{x-y} + \tilde{\xi}_2 \sin k_{x+y} + \xi_2' \sin k_{x-y}^{\mathbf{Q}} + \tilde{\xi}_2' \sin k_{x+y}^{\mathbf{Q}})$$
$$+ t_2(\xi_2 \sin k_{x+y} + \tilde{\xi}_2 \sin k_{x-y} + \xi_2' \sin k_{x+y}^{\mathbf{Q}} + \tilde{\xi}_2' \sin k_{x-y}^{\mathbf{Q}})$$
$$+ t_1(\xi_1 \sin k_x + \xi_1' \sin k_x^{\mathbf{Q}})], \tag{11}$$

with $\xi_1 = \alpha_{1,3}^{\mathbf{k,k+q}} + \alpha_{3,1}^{\mathbf{k+q,k}} + \alpha_{9,11}^{\mathbf{k+q,k}} + \alpha_{11,9}^{\mathbf{k,k+q}}$, $\xi_2 = \alpha_{1,1}^{\mathbf{k,k+q}} + \alpha_{9,9}^{\mathbf{k,k+q}}$, $\tilde{\xi}_2 = \alpha_{3,3}^{\mathbf{k,k+q}} + \alpha_{11,11}^{\mathbf{k,k+q}}$, $\xi_4 = \alpha_{1,2}^{\mathbf{k,k+q}} + \alpha_{2,1}^{\mathbf{k+q,k}} + \alpha_{9,10}^{\mathbf{k+q,k}} + \alpha_{10,9}^{\mathbf{k,k+q}}$, and $\alpha_{ij}^{\mathbf{k,k'}} = \mathbb{T}_{i,m_1}^*(\mathbf{k})\mathbb{T}_{j,m_2}(\mathbf{k'}) + \mathbb{T}_{i+1,m_1}^*(\mathbf{k})\mathbb{T}_{j+1,m_2}(\mathbf{k'})$. The corresponding ξ_i' is connected to ξ_i by changing $\alpha_{i,j}$ into $\alpha_{i+4,j+4}$. $k_{x\pm y}$ denotes $k_x \pm k_y$ and $k_{x\pm y}^{\mathbf{Q}} = k_{x\pm y} + \mathbf{Q}$. The superfluid weight measures the ratio of the superfluid density to the mass $D_s/\pi e^2 = \rho_s/m^* = -\langle J_x^Q(r_i, t)\rangle/e^2 A_x(r_i)$, and the Drude weight is a measurement of the ratio of density of mobile charges to their mass [1,33–35],

$$\frac{D_s}{\pi e^2} = \frac{1}{N}\Pi_{xx}(q_x = 0, q_y \to 0, \omega = 0) - \langle K_x\rangle_0, \tag{12}$$

$$\frac{D}{\pi e^2} = \frac{1}{N}\Pi_{xx}(q_x = 0, q_y = 0, \omega \to 0) - \langle K_x\rangle_0. \tag{13}$$

Figure 1 shows the variation of D_s, D, M and superconducting order $\Delta = \frac{1}{4}\sum_\alpha(\Delta_{i,i+\mathbf{x+y}}^\alpha + \Delta_{i,i+\mathbf{x-y}}^s)$, as functions of x at different temperatures. D does not change much as the temperature varies and we plot it clearly in Figs. 1(c) and 1(d). At zero temperature, we do not show
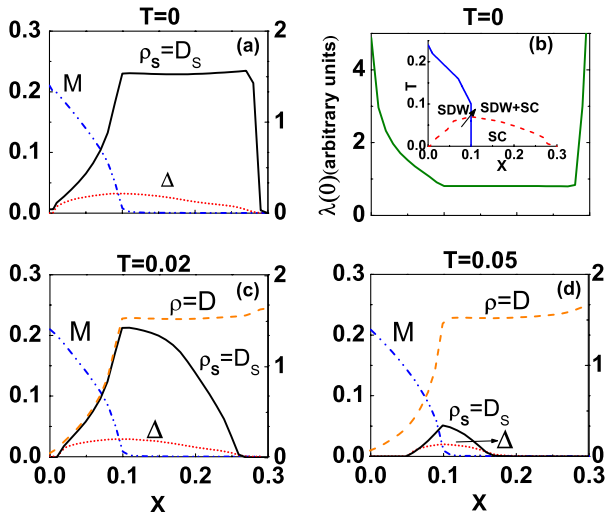
the plot of D because in almost all the doping levels $D_s = D$ as long as Δ has finite value; Fig. 1(a) shows that in the overdoped regime, the superconducting gap disappears and D_s drops to zero, while D is finite just like the plot in panels (c) and (d); hence, in the overdoped levels when $\Delta = 0$ the system corresponds to metal. We can see from Fig. 1(a) that at $T = 0$, D_s increases with the increase of x until it reaches the SDW boundary. In the underdoped region $x < 0.05$, most of the Fermi surfaces are gapped by SDW [24,29], doping is the major source of charge carrier; hence, the superfluid density as well as mobile charge density increase linearly with the increase of x. While at larger doping $0.5 < x < 0.1$, SDW is suppressed, the gapped surfaces shrinks significantly, and more intrinsic charge carriers are released to the system in addition to the doping carriers. This is the reason why the increase of $D_S = D$ with doping becomes more dramatic than the linear dependence in this region. After SDW disappears, Δ dominates the behavior of D_s, and shows a flat behavior in a considerably large doping range. In panel (b) we show the variation of $\lambda(0)$ as a function of x for $x \le 0.3$. We define $\rho_s(T) = D_s(T) = \lambda(T)^{-2}$ with arbitrary units. Compared to the phase diagram in the inset, we find that in the SDW + SC coexisting regime, $\lambda(0)$ shows a sharp increase with the decrease of x, which is in good agreement with experiments [12,13].

An external magnetic field can couple relevant correlation functions; hence, ρ_s is a nonlocal quantity, describing the stiffness of the system. Figures 1(c) and 1(d) show that at finite T, D_s deviates from D, the suppression of D_s is stronger than that of Δ. For the $U = 4$ case, the results (not shown here) are very similar to the results presented here.

Temperature dependence of superfluid density is a quantity reflecting the low-energy residual density of states inside the superconducting gap. Equation (10) indicates
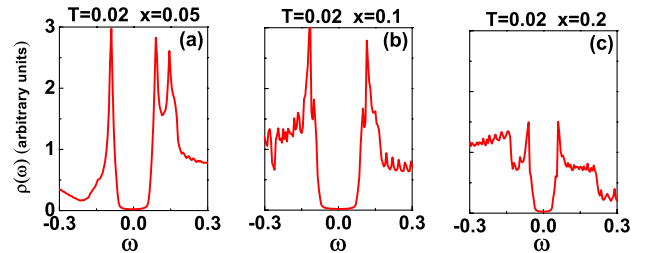

FIG. 1 (color online). Panels (a), (c), and (d) plot D_s (black solid line), D (orange dashed line), Δ (red dotted line), and M (blue dash-dot-dotted line) as functions of x at different temperatures. The right scale is for D_s and D while the left scale is for Δ and M. Panel (b) plots $\lambda(0)$ as a function of x. The inset of panel (b) is the phase diagram of temperature T and x.

FIG. 2 (color online). Density of states at $T = 0.02$ for different x. All those calculations are for the $U = 3.4$ case.
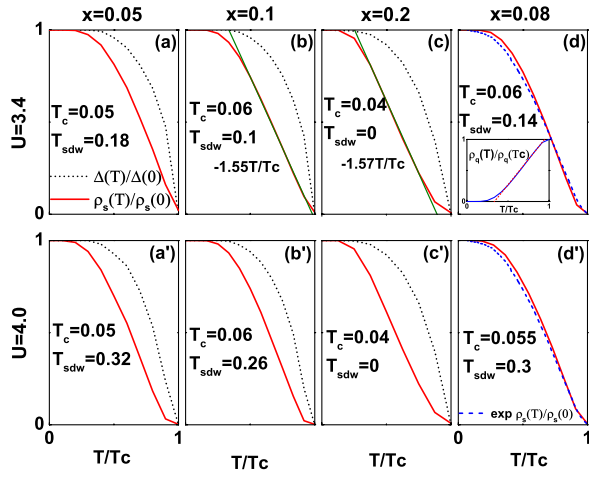
FIG. 3 (color online). Panels (a), (b), and (c) plot the renormalized superfluid density $\rho_s(T)/\rho_s(0)$ and superconducting order parameter $\Delta(T)/\Delta(0)$ as functions of the temperature T/T_c at different doping levels for $U = 3.4$. T_{sdw} is the transition temperature for SDW. The green dotted lines are linear-in-T fitting functions. Panels (a'), (b'), and (c') are similar but for $U = 4.0$. Panel (d),(d') show the comparison of our results with experiment data at $x = 0.08$. Blue solid line in the inset of panel (d') plots $\rho_q(T)/\rho(T_c)$ as a function of T/T_c at $x = 0.08$ and the red dashed line is the aid for the eyes.

that the difference between D and D_s is related to the derivation of f near the Fermi surface, and can be understood as excitation of quasiparticles ρ_q. Figure 2 shows the density of states at $T = 0.02$. For $x = 0.05$ and 0.1 the gap is considerably larger, hence D_s is equal or almost equal to D. Although there is a gap at $x = 0.2$ [see Fig. 2(c)], it is small; therefore, $f'(E_k)$ has its contribution to D_s, and therefore D_s deviates from D.

We choose three typical doping levels, to show the temperature T/T_c dependence of $\rho_s(T)/\rho_s(0)$ and $\Delta(T)/\Delta(0)$ for $U = 3.4$, as well as for $U = 4.0$. From Fig. 3 we can see that the suppression of superfluid density is stronger than that of the superconducting order parameter in all cases. At low temperatures, the curve of $\rho_s(T)/\rho_s(0)$ is flat, a characteristic of a nodeless superconducting gap.

As T increases, a linear-in-T behavior of superfluid density is dominant in all cases. For $U = 3.4$ cases, linear functions $-1.55T/T_c + 1.52$ and $-1.57T/T_c + 1.49$ are used to fit this kind of behavior for $x = 0.1$ and $x = 0.2$, respectively, which are shown in Figs. 3(b) and 3(c). It is consistent with the power-law behavior observed in the experiments [11–16]. Interestingly, they are in good agreement with the direct measurements of superfluid density in films of Fe-pnictide superconductors in Ref. [14]. We show our results and the experimental data (see Fig. 1(a) in Ref. [14]) together in Fig. 3(d) ($U = 3.4$ case) and 3(d') ($U = 4.0$ case), and their consistence is explicit. In order to understand the wider linear T dependence of $\rho_s(T)$, the
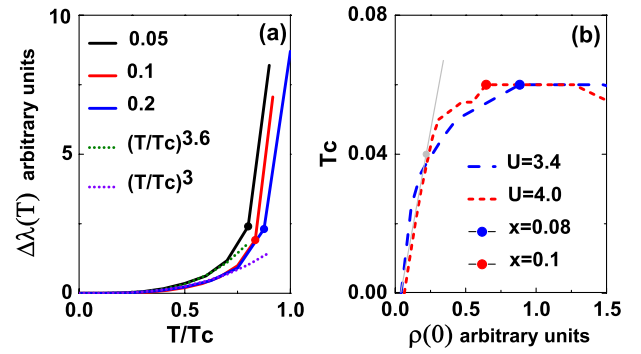

FIG. 4 (color online). Panel (a) plots $\Delta\lambda(T)$ as a function of T/T_c at typical selected doping for $U = 4$, the dashed lines are the corresponding fitting functions. Panel (b) is the Uemura plot of Fe-base superconductor. The x axis is $\rho_s(0)$ for different doping, the y axis is the corresponding T_c for the given dopings.

inset in Fig. 3(d) plots the renormalized $\rho_q(T)/\rho(T_c)$ as a function of T/T_c at $x = 0.08$; the red dashed line aids the eyes. We can see that the number of excited quasiparticles is exponentially small at low T with strong superconductivity, but it is proportional to linear T within a certain temperature range before the superconductivity disappears. The easy appearance of linear-in-T behavior is closely related to anisotropic $S_\pm$ superconducting paring, since in-gap states (Andreev states) may be induced in this case. The ratio $2\Delta_k(0)/k_BT_c$ at optimal doping is about 4.3 (4.5) for the $U = 3.4(4.0)$ system.

Experiments always measure $\Delta\lambda(T) = \lambda(T) - \lambda(0)$, so we show the evolution of $\Delta\lambda(T)$ at selected doping concentrations for $U = 4.0$ in Fig. 4(a). The results of $U = 3.4$ are very similar. In the low-temperature range the curve is flat. At high temperature approaching the disappearance of superconductivity, there is a jump for the value of $\Delta\lambda(T)$, which we show by the colored solid dots. We fit the evolution of $\Delta\lambda(T)$ to a power-law behavior. See Fig. 4(a); the corresponding fitting function $4(T/T_c)^{3.6} \times (2(T/T_c)^3)$ is for data of $x = 0.05$ ($x = 0.1, 0.2$) and it may be the reason why the experiments give different exponents for different samples.

Experiments have shown that the Uemura relation [36] holds [37] for a 1111 system but does not hold for a 122 system [38]. In Fig. 4(b), we plot T_c versus $\rho_s(0)$ based on our model. The blue-dashed line (red-dotted line) is for the $U = 3.4$ ($U = 4.0$) system. It shows that at very low doping levels, about $x < 0.035$ (grey point), both the $U = 3.4$ and $U = 4$ systems follow the same empirical linear relation (grey line). As T_c close to the maximum and $\rho_s(0)$ saturate at $x > 0.08$ (0.1) for $U = 3.4$ ($U = 4.0$), and the data significantly deviate from the linear relation. This is because in the very underdoped region the doping is a major source of charge carriers and the Uemura relation is valid here.

Based on a two-orbital phenomenological model, we have studied the stiffness of superconductivity in clean

iron-based superconductors. At zero temperature, we find $\lambda(0)$ a sharp jump as x decreases in the regime of the coexisting SDW + SC orders; the variation of $\lambda(0)$ as a function of doping is in good agreement with experiments [12]. As far as we know this is a new theoretical result. At low temperatures, $\rho_s(T)/\rho_s(0)$ is flat, then shows a linear-in-T behavior before the system loses its superconductivity. It is in good agreement with experiments of direct measurement of superfluid density in films [14]. The evolution of $\Delta\lambda(T)$ roughly follows the power-law behavior with different exponents corresponding to different doping levels. Only at low doping levels, the empirical Uemura linear relation holds for the iron-based superconductors.

[1] T. Das, J. X. Zhu, and M. J. Graf, Phys. Rev. B **84,** 134510 (2011).
[2] Y. Kamihara, T. Watanabe, M. Hirano, and H. Hosono, J. Am. Chem. Soc. **130,** 3296 (2008).
[3] X. H. Chen, T. Wu, G. Wu, R. H. Liu, H. Chen, and D. F. Fang, Nature (London) **453,** 761 (2008).
[4] J. H. Xu, J. H. Miller, and C. S. Ting, Phys. Rev. B **51,** 424 (1995).
[5] R. Prozorov and V. G. Kogan, Rep. Prog. Phys. **74,** 124 505 (2011).
[6] J. E. Sonier et al., Phys. Rev. Lett. **106,** 127002 (2011).
[7] C. Martin et al., Phys. Rev. Lett. **102,** 247002 (2009).
[8] K. Hashimoto et al., Phys. Rev. Lett. **102,** 017002 (2009).
[9] L. Malone, J. D. Fletcher, A. Serafin, and A. Carrington, Phys. Rev. B **79,** 140501(R) (2009).
[10] K. Hashimoto et al., Phys. Rev. Lett. **102,** 207001 (2009).
[11] R. T. Gordon et al., Phys. Rev. Lett. **102,** 127004 (2009).
[12] R. T. Gordon et al., Phys. Rev. B **82,** 054507 (2010).
[13] R. T. Gordon, C. Martin, H. Kim, N. Ni, M. A. Tanatar, J. Schmalian, I. I. Mazin, S. L. Bud'ko, P. C. Canfield, and R. Prozorov, Phys. Rev. B **79,** 100506(R) (2009).
[14] J. Yong, S. Lee, J. Jiang, C. Bark, J. Weiss, E. Hellstrom, D. Larbalestier, C. Eom, and T. Lemberger, Phys. Rev. B **83,** 104510 (2011).
[15] A. A. Barannik, N. T. Cherpak, N. Ni, M. A. Tanatar, S. A. Vitusevich, V. N. Skresanov, P. C. Canfield, R. Prozorov, V. V. Glamazdin, and K. I. Torokhtii, Low Temp. Phys. **37,** 725 (2011).
[16] T. J. Williams et al., Phys. Rev. B **80,** 094501 (2009).
[17] L. Luan, O. M. Auslaender, T. M. Lippman, C. W. Hicks, B. Kalisky, J. H. Chu, J. G. Analytis, I. R. Fisher, J. R. Kirtley, and K. A. Moler, Phys. Rev. B **81,** 100501 (2010).
[18] Z. Guguchia, Z. Shermadini, A. Amato, A. Maisuradze, A. Shengelaya, Z. Bukowski, H. Luetkens, R. Khasanov, J. Karpinski, and H. Keller, Phys. Rev. B **84,** 094513 (2011).
[19] L. Benfatto, M. Capone, S. Caprara, C. Castellani, and C. DiCastro, Phys. Rev. B **78,** 140502(R) (2008).
[20] R. M. Fernandes and J. Schmalian, Phys. Rev. B **82,** 014520 (2010).
[21] Y. Bang, Europhys. Lett. **86,** 47 001 (2009).
[22] A. B. Vorontsov, M. G. Vavilov, and A. V. Chubukov, Phys. Rev. B **79,** 140507(R) (2009).
[23] D. Zhang, Phys. Rev. Lett. **103,** 186402 (2009); **104,** 089702 (2010).
[24] T. Zhou, D. Zhang, and C. S. Ting, Phys. Rev. B **81,** 052506 (2010).
[25] H. Huang, D. Zhang, T. Zhou, and C. S. Ting, Phys. Rev. B **83,** 134517 (2011).
[26] Y. Gao, T. Zhou, C. S. Ting, and W. P. Su, Phys. Rev. B **82,** 104520 (2010).
[27] H. Huang, Y. Gao, D. Zhang, and C. S. Ting, Phys. Rev. B **84,** 134507 (2011).
[28] Y. Gao, H. X. Huang, C. Chen, C. S. Ting, and W. P. Su, Phys. Rev. Lett. **106,** 027004 (2011).
[29] T. Zhou, H. Huang, Y. Gao, J. X. Zhu, and C. S. Ting, Phys. Rev. B **83,** 214502 (2011).
[30] Y. Gao, J. X. Zhu, C. S. Ting, and W. P. Su, Phys. Rev. B **84,** 224509 (2011).
[31] T. Zhou, Z. Wang, Y. Gao, and C. Ting, Phys. Rev. B **84,** 174524 (2011).
[32] M. A. Tanatar, N. Ni, C. Martin, R. Gordon, H. Kim, V. Kogan, G. Samolyuk, S. Bud'ko, P. Canfield, and R. Prozorov, Phys. Rev. B **79,** 094507 (2009).
[33] D. J. Scalapino, S. R. White, and S. C. Zhang, Phys. Rev. B **47,** 7995 (1993).
[34] D. J. Scalapino, S. R. White, and S. C. Zhang, Phys. Rev. Lett. **68,** 2830 (1992).
[35] Q. Yuan, X. Z. Yan, and C. S. Ting, Phys. Rev. B **74,** 214503 (2006).
[36] Y. J. Uemura et al., Phys. Rev. Lett. **62,** 2317 (1989).
[37] H. Luetkens et al., Phys. Rev. Lett. **101,** 097009, (2008).
[38] C. Ren, Z. S. Wang, H. Q. Luo, H. Yang, L. Shan, and H. H. Wen, Phys. Rev. Lett. **101,** 257006, (2008).